

Incomplete Photonic Bandgap as Inferred from the Speckle Pattern of Scattered Light Waves

V. M. Apalkov¹, M. E. Raikh¹, and B. Shapiro²

¹Department of Physics, University of Utah, Salt Lake City, UT 84112, USA

²Department of Physics, Technion-Israel Institute of Technology, Haifa 32000, Israel

Motivated by recent experiments on intensity correlations of the waves transmitted through disordered media, we demonstrate that the speckle pattern from disordered photonic crystal with incomplete band-gap represents a sensitive tool for determination the stop-band width. We establish the quantitative relation between this width and the *angular anisotropy* of the intensity correlation function.

PACS numbers: 42.25.Dd, 42.30-d, 42.70.Qs

Introduction. A wave propagating in a random medium undergoes multiple scattering and forms a complicated intensity pattern, commonly referred to as a speckle pattern. It is described in statistical terms, with the help of probability distributions and correlation functions. The intensity correlation function, $\langle \delta I(\mathbf{r})\delta I(\mathbf{r}') \rangle$, where $\delta I(\mathbf{r})$ is the deviation from the averaged intensity at point \mathbf{r} , contains a short range term [1], $C_1(\mathbf{r}, \mathbf{r}')$, which oscillates on a scale of the wave length and exponentially decays beyond the mean free path, l . It also contains small long-range terms [2–4], which become dominant for $|\mathbf{r} - \mathbf{r}'| \gg l$. Although the theory of speckle patterns was developed some time ago, it is only recently that the first experimental measurements of the spatial correlator $C_1(\mathbf{r}, \mathbf{r}')$ were reported both for microwaves [5] and optical waves [6,7]. These experiments were carried out for *isotropic* disordered media; macroscopic isotropy was also assumed in the existing theories. In this isotropic situation comparison with the theory has enabled the authors [6] to infer the effective refractive index, which is the only relevant parameter of the medium in the absence of disorder.

The main message of this paper is that, in a medium with *underlying spatial structure*, the pattern of intensity correlations exhibits a vastly richer behavior as compared to the isotropic case. Moreover, additional features in $C_1(\mathbf{r}, \mathbf{r}')$ carry *quantitative* information about this structure. As an example, we consider a disordered incomplete-bandgap photonic crystal and demonstrate how the band-structure parameters can be extracted from the *angular anisotropy* of the correlator C_1 .

Superficially, it may seem that a wave with frequency ω , arriving from a distant source, after having been scattered by many random inhomogeneities, will lose all information about the crystal band-structure. Our point, though, is that $C_1(\mathbf{r}, \mathbf{r}')$ is essentially a *local* object: It is determined by scattering events in the vicinity of the points \mathbf{r} , \mathbf{r}' , and it is not sensitive to the “prehistory”, i.e., scattering events experienced by the wave before arrival to the point \mathbf{r} . In other words, $C_1(\mathbf{r}, \mathbf{r}')$ can serve as a “microscop” for observation of the local interference picture (on a scale smaller than l), thus, revealing the band-structure of the inherent photonic crystal. Such a microscop is particularly well suited for determination of the band-structure of *realistic* photonic crystals, since it is not affected by the long-range disorder. On the other hand, long-range disorder is a generic feature of realistic crystals, such as silica-based synthetic opals.

Disorder in synthetic opals. Silica-based synthetic opals, which are the fcc self-assembled arrangement of almost monodispersed silica spheres, play a distinguished role in fabrication of photonic band gap materials, the potential of which for light manipulation was first appreciated in Refs. [8,9]. This is because the opals constitute a template subsequently infiltrated with high refraction index material, while the spheres are selectively removed (see *e.g.* [10–12]). Due to this distinguished role, the vast majority of experimental studies of light propagation in photonic crystals has been carried out on opals [13].

In opal photonic crystals, the contrast of the dielectric constant is weak, so that photonic bandgaps are not only incomplete, but the corresponding stop-bands are relatively narrow. For this reason, the photonic band structure of this materials is strongly obscured by the disorder. As a result, any reliable determination of the stop-band either from disorder-broadened reflection maxima or from transmission minima, which are also strongly affected by the disorder, is highly ambiguous. In fact, in early studies, actual extraction of the stop-band width from the data was based on the “thumb rules” [14,15].

Later studies [13,16–18] have yielded a deeper insight into the microscopic origin of the disorder in opals. Namely, they indicated that one should distinguish three types of the disorder

- (i) Short-range disorder due to point defects and spread in the sphere diameters. This type of the disorder causes the mean free path [19] $l \sim 15\mu\text{m}$.
- (ii) Stacking faults in [111] direction [16]. This disorder has a *one-dimensional* character, and thus might give rise to the

1D in-gap states [20] within the incomplete stop-band. In fact, experimentally observed deep and sharp transmission minimum [16] near the stop-band center has been accounted for these states. Subsequent interpretation of reflection and transmission [17] as well as diffraction data [18] also relied on the prominent role played by the stacking faults. (iii) macroscopic domains that are $\sim 50 - 100\mu\text{m}$ in size. Such domains unavoidably emerge in course of self-assembly of thick enough photonic crystals [13]. Due to their presence the stop-bands are strongly *inhomogeneously* broadened – a serious complication for determination of photonic band structure.

Summarizing, experimental studies [13,16–18] have led to significant improvement of the understanding of the light propagation in strongly-disordered incomplete-bandgap photonic crystals. However, no quantitative information about the stop-band width could be inferred from these experiments. Below we demonstrate that this width naturally emerges in the *angular dependence* of the intensity correlator C_1 .

Correlator C_1 in a disordered photonic crystal. The short-range correlator $C_1(\mathbf{r}, \mathbf{r}')$, is obtained by factorizing the product of four fields $\psi(\mathbf{r})$ in the average $\langle I(\mathbf{r})I(\mathbf{r}') \rangle$. This leads [2] to the relation $C_1(\mathbf{r}, \mathbf{r}') = |C_\psi(\mathbf{r}, \mathbf{r}')|^2$, where

$$C_\psi(\mathbf{r}, \mathbf{r}') = \frac{\langle \psi(\mathbf{r})\psi^*(\mathbf{r}') \rangle}{\langle I(\mathbf{r}) \rangle^{1/2} \langle I(\mathbf{r}') \rangle^{1/2}} \quad (1)$$

is the field correlation function. It follows from the Bethe-Salpeter equation that

$$C_\psi(\mathbf{r}, \mathbf{r}') = \frac{4\pi}{l} \int d\mathbf{r}_1 \langle G(\mathbf{r}, \mathbf{r}_1) \rangle \langle G^*(\mathbf{r}', \mathbf{r}_1) \rangle, \quad (2)$$

where $\langle G(\mathbf{r}, \mathbf{r}_1) \rangle$ is the disorder-averaged Green's function. The physical meaning of Eq. (2) is that correlation between points \mathbf{r} , \mathbf{r}' is established via scattering on an intermediate impurity, at \mathbf{r}_1 . The integral Eq. (2) can be reduced to

$$C_\psi(\mathbf{r}, \mathbf{r}') = -\frac{4\pi c^3}{\epsilon^{3/2}\omega} \text{Im} \langle G(\mathbf{r}, \mathbf{r}') \rangle, \quad (3)$$

which has the following intuitive explanation: field correlation between a pair of points is due primarily to waves that are scattered in the vicinity of one point and arrive to the vicinity of the other point. The average amplitude to arrive from \mathbf{r}' to \mathbf{r} is $\langle G(\mathbf{r}, \mathbf{r}') \rangle$, so that $C_\psi(\mathbf{r}, \mathbf{r}')$ should be a linear combination of $\langle G(\mathbf{r}, \mathbf{r}') \rangle$ and $\langle G^*(\mathbf{r}, \mathbf{r}') \rangle$. Eq. (3) is the right linear combination since it reduces to unity for $\mathbf{r} = \mathbf{r}'$. Using Eq. (3) we present the field correlator as

$$C_\psi(\mathbf{r}, \mathbf{r}') = -\frac{4\pi c^3}{\epsilon^{3/2}\omega} \text{Im} \sum_{\mu, \mathbf{k}} \frac{\psi_{\mu, \mathbf{k}}(\mathbf{r})\psi_{\mu, \mathbf{k}}^*(\mathbf{r}')}{\omega^2 - \omega_{\mu, \mathbf{k}}^2 + i\eta}, \quad (4)$$

where $\eta = c\omega/\epsilon^{1/2}l$, with ϵ standing for the background dielectric constant, and $\psi_{\mu, \mathbf{k}}^*(\mathbf{r})$, $\omega_{\mu, \mathbf{k}}$ are the photonic crystal eigenmodes and eigenfrequencies, respectively. They are characterized by the wave vector \mathbf{k} of the first Brillouin zone and the band index $\mu = \pm 1$.

Suppose that stop-band corresponds to the direction of propagation along the z -axis. Then, the anisotropy of $C_\psi(\mathbf{r}, \mathbf{r}')$ is expected within a narrow angular interval, $\theta = \arctan(z' - z)/(\rho' - \rho) \sim \gamma^{1/2}$, where $\gamma = \delta\omega/\omega \ll 1$ is the dimensionless frequency width of the stop-band. For such θ , the main contribution to the sum in Eq. (4) comes from the small domain of \mathbf{k} -space around the Bragg condition $k_z \approx Q_B/2$, where $2\pi/Q_B$ is the period along z (see Fig. 1). Within this domain the dispersion law, $\omega_{\mu, \mathbf{k}}$, can be simplified as

$$\frac{\epsilon\omega_{\mu, \mathbf{k}}^2}{c^2} = k_\perp^2 + \frac{Q_B^2}{4} + \mu Q_B \sqrt{\frac{1}{L_B^2} + \left(k_z - \frac{Q_B}{2}\right)^2}, \quad (5)$$

where we have introduced the Bragg length, $L_B = 4\omega/Q_B\delta\omega$, of the decay along z exactly at the Bragg condition. The corresponding eigenmodes, $\psi_{\mu, \mathbf{k}}$ can be also simplified

$$\psi_{\mu, \mathbf{k}} = \mathcal{U}_\mu(z) \exp[i(k_z - Q_B/2)z + i\mathbf{k}_\perp \boldsymbol{\rho}], \quad (6)$$

where \mathcal{U}_μ are the Bloch functions. It is seen from Eq. (5) that, for a given $\omega_{\mu, \mathbf{k}} = \omega$ and the same k_z , the values of k_\perp are very different for upper $\mu = 1$ and lower $\mu = -1$ bands. As a result, the contribution to C_ψ from the upper band is exponentially smaller. Then, keeping only $\mu = -1$ terms, we can express the field-field correlation function as

$$C_\psi(\mathbf{r}, \mathbf{r}') = -\frac{c^3 \mathcal{U}_{-1}(z)\mathcal{U}_{-1}(z')}{2\pi^3 \epsilon^{3/2}\omega} \int dk_z \int k_\perp dk_\perp \int d\phi \text{Im} \left\{ \frac{\exp[iz(k_z - Q_B/2) + i\rho k_\perp \cos \phi]}{\omega^2 - \omega_{-1, \mathbf{k}}^2 + i\eta} \right\}. \quad (7)$$

Substituting Eq. (5) into the integral Eq. (7), and performing the integration over k_\perp and ϕ we arrive at

$$C_\psi(\mathbf{r}, \mathbf{r}') = \left(\frac{\gamma}{4}\right) \mathcal{U}_{-1}(z) \mathcal{U}_{-1}(z') \operatorname{Re} \left\{ \int dq \exp \left[i q \frac{\gamma \mathcal{R}}{4} \right] H_0 \left(\frac{\theta \mathcal{R} \gamma^{1/2}}{2} \sqrt{\Delta + \sqrt{1 + q^2}} \right) \right\}, \quad (8)$$

where H_0 is a Hankel function of a zero order. The dimensionless length \mathcal{R} and “detuning” Δ are defined as

$$\mathcal{R} = |\mathbf{r} - \mathbf{r}'| Q_B, \quad \Delta = \frac{2}{\delta\omega} \left(\omega - \frac{cQ_B}{2\epsilon^{1/2}} \right) + i \frac{L_B}{2l}. \quad (9)$$

For $\theta \mathcal{R} \gamma^{1/2} \gg 1$, i.e. $|\mathbf{r} - \mathbf{r}'| \gg L_B$, the asymptotic expansion of the Hankel function can be used, so that the integral Eq. (8) takes the form

$$C_\psi(\mathbf{r}, \mathbf{r}') = \mathcal{U}_{-1}(z) \mathcal{U}_{-1}(z') \left[\frac{\gamma^{3/4}}{2(\pi \mathcal{R})^{1/2}} \right] \operatorname{Re} \left\{ e^{-i\pi/4} \int dq \frac{\exp[i\mathcal{R}F(\theta, q)]}{(\Delta + \sqrt{1 + q^2})^{1/4}} \right\}, \quad (10)$$

where $F(\theta, q) = \gamma q/4 + \theta(\gamma^{1/2}/2) [\Delta + \sqrt{1 + q^2}]^{1/2}$. Function $F(\theta, q)$ has a special point at which the first and the second derivatives with respect to Q , for some value of $\theta = \theta_c$, are zero. The position of this critical point, (θ_c, q_c) , depends on the detuning Δ and can be parametrized by a complex number w as

$$\Delta = \frac{4}{27} w^3 - w, \quad \theta_c = 2\gamma^{1/2} \left(\frac{w}{3}\right)^{3/2}, \quad q_c = \frac{1}{3} (4w^2 - 9)^{1/2}$$

For $\Delta = 0$ we have $w = 3^{3/2}/2$, $\theta_c = (3^{3/4}/2^{1/2})\gamma^{1/2}$, and $q_c = 2^{1/2}$. To evaluate the integral Eq. (10) for θ close to the critical point, $\theta \sim \theta_c$, the function $F(\theta, q)$ should be expanded up to the third order in $(q - q_c)$

$$F(\theta, q) = \phi_0 + \frac{\delta\theta}{\theta_t} + \delta q \frac{\delta\theta}{\theta_d} - \frac{1}{3} (\delta q)^3, \quad (11)$$

where $\delta\theta = \theta - \theta_c$, $\delta q = (9/4w)(6/w)^{1/3}(q - q_c)$, $F_0 = \gamma(4w^2 - 9)^{3/2}/108$, and characteristic angles θ_t and θ_d are defined as

$$\theta_t = \frac{6}{\gamma^{1/2}} \left(\frac{3}{4w^3 - 9w} \right)^{1/2}, \quad \theta_d = 6 \left(\frac{2w}{3\gamma} \right)^{1/6}. \quad (12)$$

Substituting Eq. (11) into Eq. (10) and performing integration over δq , we obtain

$$C_\psi(\mathbf{r}, \mathbf{r}') = \left[\frac{2\gamma^{1/5}}{3\mathcal{R}} \right]^{5/6} \mathcal{U}_{-1}(z) \mathcal{U}_{-1}(z') \operatorname{Re} \left\{ \frac{\pi^{1/2} w^{1/3}}{(4w^2 - 9)^{1/4}} \exp \left(i\phi_0 + i\mathcal{R} \frac{\delta\theta}{\theta_t} \right) Ai \left(-\mathcal{R}^{2/3} \frac{\delta\theta}{\theta_d} \right) \right\}, \quad (13)$$

where Ai is the Airy function.

Discussion. It is easy to see that Eq. (13) has a form similar to the field distribution near the caustics, which is the envelope of rays reflected by a curved surface [21]. This similarity is not accidental. Indeed, near the caustics the light rays cross over from geometrically allowed directions to the “shadow”. Eq. (13) also describes a crossover from the directions $\theta \gg \theta_c \sim \gamma^{1/2}$ of free propagation to the angular domain $\theta \lesssim \gamma^{1/2}$ where propagation is forbidden due to the stop-band, which plays the role of “shadow” in the \mathbf{k} -space. Similarly to the case of caustics, the behavior of C_ψ near the crossover $\theta = \theta_c$ is described by the following exponential decay at $\theta < \theta_c$

$$C_\psi(\theta) \sim \exp \left[-\mathcal{R} \left(\frac{\theta_c - \theta}{\theta_d} \right)^{3/2} \right] \cos \left[\mathcal{R} \frac{\theta_c - \theta}{\theta_t} + \phi_0 \right],$$

which, in the case of intensity correlation serves as an envelope of the fast oscillations. For $\theta > \theta_c$ this envelope oscillates itself as $\cos \left[\mathcal{R} \left(\frac{\theta - \theta_c}{\theta_d} \right)^{3/2} - \pi/4 \right]$. Overall, there are three angular scales in the correlator C_ψ , namely, the critical angle, θ_c , the period of the envelope, $\theta_d/\mathcal{R}^{2/3}$, and the period, θ_t/\mathcal{R} , of the oscillations. At spatial distances $|\mathbf{r} - \mathbf{r}'| \sim L_B$ all three scales are of the same order $\sim \gamma^{1/2}$. For large $|\mathbf{r} - \mathbf{r}'|$ we have $\theta_c \gg \theta_d/\mathcal{R}^{2/3} \gg \theta_t/\mathcal{R}$.

Numerical examples, illustrating separation of the three scales is given in Fig. 2. Outside the stop-band, $\theta \gg \gamma^{1/2}$ the correlator C_1 saturates at the value $\propto \exp(-|\mathbf{r} - \mathbf{r}'|/l)$, governed by the mean free path [1]. Obviously, our main result Eq. (13) applies in the vicinity of each of the equivalent Bragg directions.

When large-scale disorder (domains) broadens significantly the reflectivity peak, $\mathbf{R}(\theta)$, the dependence $C_1(\theta)$ with all fine details *remains unchanged*. Even if disorder is purely short-range, the intensity correlations are much more sensitive to the periodic background than the reflectivity. To illustrate this, in Fig. 3 we present the dependence $C_1(\theta)$ together with $\mathbf{R}(\theta)$, which near the Bragg condition is given by

$$\mathbf{R} = \left| \frac{\epsilon^{1/2} - 1 + (\epsilon^{1/2} + 1) \left[g(\theta) - \sqrt{1 + g^2(\theta)} \right]}{\epsilon^{1/2} + 1 + (\epsilon^{1/2} - 1) \left[g(\theta) - \sqrt{1 + g^2(\theta)} \right]} \right|^2, \quad (14)$$

where $g(\theta) = L_B/2l + 4i\theta^2/\epsilon\gamma$. The dependencies $\mathbf{R}(\theta)$, $C_1(\theta)$ were calculated for the effective refractive index $\epsilon^{1/2} = 1.7$ and $L_B = l$. Similar to C_1 , the width of $\mathbf{R}(\theta)$ is $\theta \sim \gamma^{1/2}$. However, $\mathbf{R}(\theta)$ is strongly smeared when $L_B = l$, whereas $C_1(\theta)$ contains oscillations. Three oscillations are well pronounced for the distances $|\mathbf{r} - \mathbf{r}'|$ equal to $2l$, and $3l$, as shown in Fig. 3. Since these values are comparable to L_B , the argument of the Hankel function in Eq. (8) is ~ 1 . Therefore, $C_1 = |C_\psi|^2$ was calculated directly from (8) without using the asymptotical form Eq. (10). Therefore, even when $L_B \sim l$, comparison of the saturation values of $C_1(\theta)$ at two $|\mathbf{r} - \mathbf{r}'|$ allows to determine the value of the mean free path. Then L_B and, correspondingly, the stop-band width, $\delta\omega = 2c/\epsilon^{1/2}L_B$, can be inferred from the oscillations in the following way. Knowledge of the oscillation period, $\pi\theta_t(w)/\mathcal{R}$ together with frequency and mean free path, allows to deduce the parameter w , then the detuning Δ , defined by Eq. (9), and, finally, $L_B = 2l \{\text{Im}\Delta\}$.

Conclusion. In the present paper we have demonstrated that the intensity correlations in a disordered photonic crystal with *incomplete* bandgap uncover the underlying band structure that is obscured by the disorder, so that conventional approaches applicable to the “clean” photonic crystals [22,23] fail.

It is important to emphasize that the very phenomenon of intensity correlation is a *disorder induced* effect and that the function $C_1(\mathbf{r}, \mathbf{r}')$ is calculated under the condition of diffusive propagation of the wave inside the sample. Note that, conceptually, with C_1 playing the role of a microscope, there is an analogy between the correlation of the fluctuations and the experimental setup [24–26], in which the source of light is located inside the crystal and the directionality of the outgoing light is studied. On the contrary, the long-range contributions [2,3] to the intensity correlator come from scattering trajectories that explore *all* directions inside the crystal, and, due to isotropization, do not carry information about the Bragg directions.

Note in conclusion, that sensitivity of a number of disorder-induced effects, such as coherent backscattering [19,27] and directionality of the exiting diffusing light [28], to the periodic background has already been discussed in the literature. This sensitivity has also been employed [19,28] for the estimation of the stop-band width. In this regard, the intensity correlations constitute a much more accurate tool. Indeed, in the shape of the coherent backscattering cone, the properties of periodic structure enter only through the convolution with cooperon, which describes the large-scale diffusive motion, whereas the correlator C_1 comes from *short distances*. Another advantage of using intensity correlations over traditional methods is that C_1 is insensitive to the long-range disorder due to domains that mask the photonic band structure [13]. Earlier it was demonstrated [29] that, isolating a single domain and measuring reflection from this domain, results in a drastic narrowing of the reflection spectra. We emphasize, that correlation analysis of the speckle pattern allows to get rid of inhomogeneous broadening in a natural way.

Finally, an attractive avenue for the future work comes from proposed infiltrating opals with nematic liquid crystals to manipulate the photonic band gap externally [30]. While in reflectivity measurements reorientation of the nematic director manifests itself in a simple shift of the optical Bragg reflection peak [31], the structure of the correlator C_1 might reveal the effect of birefringence on the photonic bandstructure.

Acknowledgements. One of the authors (B.S.) acknowledges the hospitality of the University of Utah. The work was supported by the Army Research Office under grant No. DAAD 19-03-1-0290 and by the Petroleum Research Fund under grant No. 37890-AC6.

[1] B. Shapiro, Phys. Rev. Lett. **57**, 2168-2171 (1986).

[2] M. J. Stephen and G. Cwilich, Phys. Rev. Lett. **59**, 285 (1987).

- [3] S. Feng, C. Kane, P. A. Lee, and A. D. Stone, Phys. Rev. Lett. **61**, 834 (1988).
- [4] E. Akkermans and G. Montambaux, in *Mesoscopic Physics of Electrons and Photons*, EDP Sciences-CNRS (2004), in press.
- [5] P. Sebbah, B. Hu, A. Z. Genack, R. Pnini, and B. Shapiro Phys. Rev. Lett. **88**, 123901 (2002).
- [6] V. Emiliani, F. Intonti, M. Cazayous, D. S. Wiersma, M. Colocci, F. Aliev, and A. Lagendijk, Phys. Rev. Lett. **90**, 250801 (2003).
- [7] A. Apostol and A. Dogariu, Phys. Rev. Lett. **91**, 093901 (2003).
- [8] E. Yablonovitch, **58**, 2059 (1987).
- [9] S. John, Phys. Rev. Lett. **58**, 2486 (1987).
- [10] J.E.G.J. Wijnhoven and W.L. Vos, Science **281**, 802 (1998).
- [11] A. A. Zakhidov, R. H. Baughman, Z. Iqbal, C. Cui, I. Khairulin, S. O. Dantas, J. Marti, and V. G. Ralchenko, Science **282**, 897 (1998).
- [12] A. Blanco, E. Chomski, S. Grabtchak, M. Ibisate, S. John, S. W. Leonard, C. Lopez, F. Meseguer, H. Miguez, J. P. Mondia, G. A. Ozin, O. Toader, and H. M. van Driel, Nature (London) **405**, 437 (2000).
- [13] Extensive literature on the subject can be found in V. N. Astratov, A. M. Adawi, S. Fricker, M. S. Skolnick, D. M. Whittaker, and P. N. Pusey, Phys. Rev. B **66**, 165215 (2002).
- [14] W. L. Vos, M. Megens, C. M. van Kats, and P. Bosecke, J. Phys. Condens. Matter **8**, 9503 (1996)
- [15] I. I. Tarhan and G. H. Watson, Phys. Rev. Lett. **76**, 315 (1996).
- [16] Yu. A. Vlasov, M. A. Kaliteevski, and V. V. Nikolaev, Phys. Rev. B **60**, 1555 (1999).
- [17] Yu. A. Vlasov, V. N. Astratov, A. V. Baryshev, A. A. Kaplyanskii, O. Z. Karimov, and M. F. Limonov Phys. Rev. E **61**, 5784 (2000).
- [18] A. V. Baryshev, A. A. Kaplyanskii, V. A. Kosobukin, M. F. Limonov, K. B. Samusev, and D. E. Usvyat, Phys. Solid State **45**, 459 (2003).
- [19] J. Huang, N. Eradat, M. E. Raikh, Z. V. Vardeny, A. A. Zakhidov, and R. Baughman, Phys. Rev. Lett. **86**, 4815 (2001).
- [20] L. I. Deych, D. Zaslavsky, and A. A. Lisyansky, Phys. Rev. Lett. **81**, 5390 (1998).
- [21] L.D. Landau and E. M. Lifshitz, *The Classical Theory of Fields*, Pergamon Press, Oxford, 1980.
- [22] J. F. Bertone, P. Jiang, K. S. Hwang, D. M. Mittleman, and V. L. Colvin Phys. Rev. Lett. **83**, 300 (1999); J. F. Galisteo-López, E. Palacios-Lidón, E. Castillo-Martinez, and C. López, Phys. Rev. B **68**, 115109 (2003).
- [23] M. S. Thijssen, R. Sprik, J. E. G. J. Wijnhoven, M. Megens, T. Narayanan, Ad Lagendijk, and W. L. Vos, Phys. Rev. Lett. **83**, 2730 (1999).
- [24] E. P. Petrov, V. N. Bogomolov, I. I. Kalosha, and S. V. Gaponenko, Phys. Rev. Lett. **81**, 77 (1998).
- [25] S. G. Romanov, T. Maka, and C. M. Sotomayor Torres M. Müller, and R. Zentel, J. Appl. Phys. **91**, 9426 (2002).
- [26] A. F. Koenderink, L. Bechger, H. P. Schriemer, A. Lagendijk, and W. L. Vos, Phys. Rev. Lett. **88**, 143903 (2002).
- [27] A. Yu. Sivachenko, M. E. Raikh, and Z. V. Vardeny, Phys. Rev. B **63**, 245103 (2001).
- [28] A. F. Koenderink and W. L. Vos, Phys. Rev. Lett. **91**, 213902 (2003).
- [29] Yu. A. Vlasov, M. Deutch, and D. J. Norris, Appl. Phys. Lett. **76**, 1627 (2000); Y. A. Vlasov, X. Z. Bo, J. C. Sturm, and D. J. Norris, Nature (London) **414**, 289 (2001).
- [30] K. Busch and S. John, Phys. Rev. Lett. **83**, 967 (1999).
- [31] D. Kang, J. E. Maclennan, N. A. Clark, A. A. Zakhidov, and R. H. Baughman, Phys. Rev. Lett. **86**, 4052 (2001).

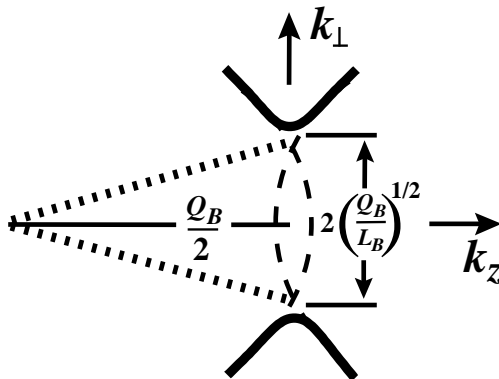


FIG. 1. Surface of constant frequency $\omega(k_z, k_\perp) = \omega$ is shown schematically for the Bragg frequency $\omega = cQ_B/2\epsilon^{1/2}$

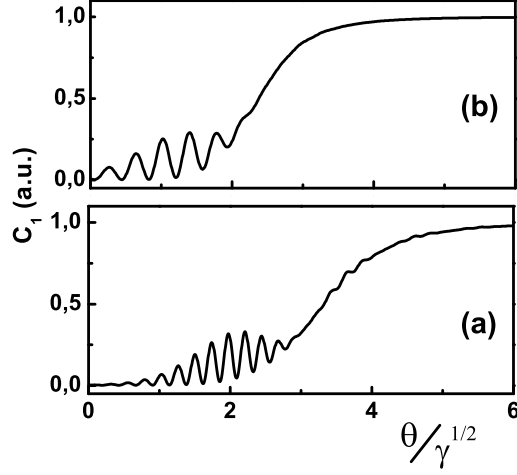


FIG. 2. Correlator C_1 as a function of dimensionless angle $\theta/2(Q_B L_B)^{-1/2}$ is shown for $|\mathbf{r} - \mathbf{r}'| = 5L_B$ and for two dimensionless “detunings”, Δ , defined by Eq. (9); (a) $\Delta = 0.15i$ (i.e., frequency is equal to the Bragg frequency and $L_B = 0.3l$); (b) $\Delta = 0.5 + 0.15i$.

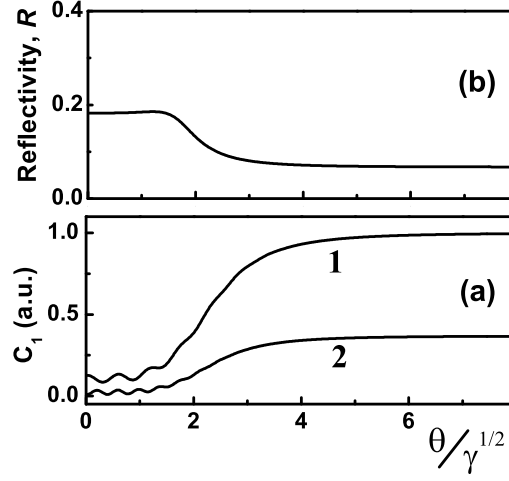


FIG. 3. (a) Correlator C_1 as a function of dimensionless angle $\theta/2(Q_B L_B)^{-1/2}$ is shown for $L_B = l$ and two distances $|\mathbf{r} - \mathbf{r}'| = 2l$ (curve 1) and $|\mathbf{r} - \mathbf{r}'| = 3l$ (curve 2); (b) Angular dependence of the reflectivity is shown for $L_B = l$ and effective refractive index $\epsilon^{1/2} = 1.7$.